

REPUBLIC OF AZERBAIJAN

On the right of the manuscript

ABSTRACT

of the dissertation for the degree of Doctor of Philosophy

**PHYSICOCHEMICAL STUDY OF THE $\text{Ag, B}^{\text{IV}}\|\text{X, Te}$
($\text{B}^{\text{IV}}\text{-Si, Ge, X-S, Se}$) RECIPROCAL SYSTEMS**

Speciality: 2303.01 – Inorganic chemistry

Field of science: Chemistry

Applicant: **Amiraslanova Aynura Jabbar**

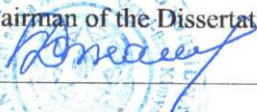
Baku – 2025

The dissertation work was performed in the Chemistry department of Ganja State University of the Ministry of Science and Education of the Republic of Azerbaijan.


- Scientific supervisor: Doctor of chemistry, professor
Yusif Amirali Yusibov
- Scientific consultant: Corr.-member of ANAS, professor
Mahammad Baba Babanlı
- Official opponents: Doctor of chemistry, professor
Ozbek Misirkhan Aliev
Doctor of chemistry, professor
Huseyn Ramazan Gurbanov
PhD in chemistry
Guntekim Miralam Shukurova

Dissertation Council ED 1.15 of Supreme Attestation Commission under the President of the Republic of Azerbaijan operating in the Institute of Catalysis and Inorganic Chemistry named after acad. M.Nagiyev of the Ministry of Science and Education of the Republic of Azerbaijan

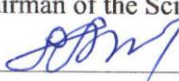
Chairman of the Dissertation Council:


D.Chem.Sci., academician
Dilgam Tagiyev Babir

Scientific Secretary of the Dissertation Council:


PhD in chemistry, associate prof.
Ulviyya Mammadova Ahmed

Chairman of the Scientific Seminar:


D.Chem.Sci., prof.
Akif Aliyev Shikhan

GENERAL DESCRIPTION OF WORK

Relevance and degree of investigation of the topic. Modern scientific and technological progress is largely associated with the application of new functional materials with unique properties. This requires a systematic search, synthesis, design, and detailed study of the properties of such materials. Currently, alternative energy problems are one of the most priority areas of scientific research all over the world. The solution to this problem is closely related to the creation of new efficient energy converters, in particular, thermoelectric and photovoltaic materials.

Transition metal chalcogenides, including copper and silver, are among the most suitable base compounds for the creation of new environmentally safe functional materials. Many of them have high thermoelectric efficiency, and interesting photoelectric, optical, and magnetic properties, and are used in modern energy conversion devices or are promising for application¹.

Among the complex chalcogenides of copper and silver, the argyrodite family compounds occupy a special place. Most of these compounds have polymorphic phase transitions at relatively low (≤ 530 K) temperatures. While low-temperature modifications have various types of crystal lattices, high-temperature modifications crystallize in a cubic (Sp.gr. $F-43m$) structure. During the polymorphic transition, the rigid anion skeleton is deformed and the compounds pass into high-temperature phases with a more disordered structure. In these phases, the A+ cations are in relatively weak chemical bonds with the anion skeleton. Since their positions in the cation sublattice are more than twice the number of Cu^+ (Ag^+) cations, they are mobile as in liquids. This property leads to the high ionic conductivity and anomalously low thermal conductivity of the argyrodite family compounds².

¹ Chalcogenides: Advances in Research and Applications: / ed.P.Woodrow. - Nova Science Publisher, - 2018. - 103p

² Lin S., Li W., Pei Y. Thermally insulative thermoelectric argyrodites // Materials Today, - 2021. vol. 48, - p. 198-213

On the other hand, all argyrodite family compounds are crystalline semiconductors and have high electrical conductivity. This makes them very attractive as thermoelectric materials. The crystal structure characteristics of these compounds also lead to them having several other functional properties, in particular, high photoelectric and optical indicators. Argyrodite family compounds and phases based on them, in addition to their interesting electronic properties, are also considered very promising for applications such as electrochemical sensors, ion batteries, and ion-selective electrodes, since they have high ionic conductivity³.

One of the most effective ways to create a physicochemical basis for the search and production of new multicomponent materials, including phases based on the argyrodite family compounds, is the study of phase equilibria in the relevant systems. The phase diagram allows not only to detect new compounds and phases with variable composition in the system, but also to determine their crystallization properties from the alloy, thermal stability, homogeneity zones, and phase transformations, which is extremely important for solving problems such as directed synthesis and crystal growth⁴.

To obtain solid solutions based on known argyrodite compounds, four-component and more complex systems consisting of silver (copper) and p²-element chalcogenides should be studied.

An analysis of the literature shows that although considerable work has been done in the field of studying systems of this type in the last decade, research on silica argyrodites is almost non-existent.

Object and subject of research. Taking into account the above,

³ Pogodin A.I., Filep M., Malakhovska T. et al. Recrystallization effect on mechanical parameters and increasing of Ag⁺ ionic conductivity in Ag₇(Si_{1-x}Ge_x)S₅I ceramic materials // Solid State Sciences, - 2023. vol. 140, - p 107203

⁴ M.B.Babanly, L.F.Mashadiyeva, D.M.Babanly et al Some issues of complex investigation of the phase equilibria and thermodynamic properties of the ternary chalcogenide systems by the EMF method // Russian Journal of Inorganic Chemistry, - 2019. 64(13), - p.1649-1671

the $\text{Ag}_2\text{X}-\text{Ag}_8\text{B}^{\text{IV}}\text{Te}_6-\text{Ag}_8\text{B}^{\text{IV}}\text{X}_6-\text{Ag}_2\text{Te}$ composition planes of the $\text{Ag}-\text{B}^{\text{IV}}-\text{Te}-\text{X}$ (B - Si, Ge; X - S, Se) quaternary systems were taken as the objects of research of the dissertation work. The subject of the research was the study of phase equilibria and thermodynamic properties of some phases on these planes.

The aim and tasks of the study. The main aim of the dissertation work was to obtain reliable schemes of phase equilibria in the $6\text{Ag}_2\text{X}+\text{Ag}_8\text{B}^{\text{IV}}\text{Te}_6\leftrightarrow 6\text{Ag}_2\text{Te}+\text{Ag}_8\text{B}^{\text{IV}}\text{X}_6$ reciprocal systems and to obtain new anion-substituted argyrodite phases.

To achieve this aim, the following specific issues were set and resolved:

➤ Determination of the nature of the physicochemical interaction at the boundary systems of the $6\text{Ag}_2\text{X}+\text{Ag}_8\text{B}^{\text{IV}}\text{Te}_6\leftrightarrow 6\text{Ag}_2\text{Te}+\text{Ag}_8\text{B}^{\text{IV}}\text{X}_6$ mutual systems, consisting of compounds of the argyrodite family, obtaining new solid solutions using anion exchange, determining the nature of their formation, areas of homogeneity and phase transitions;

➤ construction of various vertical and horizontal sections of phase diagrams of these mutual systems, as well as projections of liquidus surfaces;

➤ synthesis of various compositional samples of the discovered variable composition phases, determination of their crystal lattice types and parameters;

➤ determination of thermodynamic functions of the Ag_8GeTe_6 compound and $\text{Ag}_8\text{GeS}_{6-x}\text{Te}_x$ solid solutions by the EMF method with Ag^+ conductive solid electrolyte.

Research methods. The research on the topic of the dissertation was carried out using differential thermal analysis (DTA), X-ray phase analysis (XRD), scanning electron microscopy (SEM), and electromotive forces (EMF) methods. DTA was carried out using a "Termoscan-2" pyrometer, a NETZSCH 404 F1 Pegasus device, as well as a multi-channel DTA device assembled based on an electronic data recorder "TC-08 Thermocouple Data Logger". Powder diffractograms were taken on D8 ADVANCE and D2 Phaser devices of the German company Bruker and analyzed using com-

puter software for the corresponding diffractometers. SEM images were obtained using a JEOLJSM-7600F scanning electron microscope. EMF measurements were carried out using a Keithley 2100 6 ½ high-resistance multimeter.

Provisions submitted for defense

1. New schemes of phase equilibria in the $6\text{Ag}_2\text{X}+\text{Ag}_8\text{B}^{\text{IV}}\text{Te}_6\leftrightarrow 6\text{Ag}_2\text{Te}+\text{Ag}_8\text{B}^{\text{IV}}\text{X}_6$ reciprocal systems, a number of poly- and isothermal sections of volume phase diagrams, projections of liquidus surfaces, types and coordinates of non- and monovariant equilibria.

2. New variable composition phases discovered in the studied systems, their primary crystallization surfaces from the liquid, homogeneity areas and crystallographic parameters.

3. Partial and standard integral thermodynamic functions of the Ag_8GeTe_6 compound and $\text{Ag}_8\text{GeS}_{6-x}\text{Te}_x$ solid solutions determined by the EMF method.

Scientific novelty of the research. The following new scientific results were obtained in the dissertation work:

- The character of the physicochemical interaction of the Ag-Si(Ge)-Te-S(Se) systems on the sections consisting of argyrodite family compounds was determined. It was shown that in silicon systems these sections are quasi-binary, while in germanium systems they are non-quasi-binary due to the incongruent melting of the Ag_8GeTe_6 compound. In all these systems, continuous solid solutions are formed between the high-temperature modifications of the initial ternary compounds;

- in three of the studied reciprocal systems - Ag, Si || S(Se), Te and Ag, Ge || Se, Te systems, complete schemes of the phase equilibria were obtained, a number of polythermal and isothermal sections of their phase diagrams, as well as projections of liquidus surfaces were constructed. For the Ag, Ge || S, Te system, the nature of solid-phase equilibria was determined.

- in the studied systems, wide solid solution areas were discovered based on binary and ternary compounds, their homogeneity and initial crystallization areas were determined, and solid solu-

tion samples with different compositions were synthesized and identified;

- partial molar functions of silver in the Ag_8GeTe_6 compound and $\text{Ag}_8\text{GeS}_{6-x}\text{Te}_6$ solid solutions and standard integral thermodynamic functions of these phases were determined by the solid electrolyte EQ method;

The theoretical and practical significance of the research.

The *scientific and theoretical significance* of the results obtained in the dissertation work is that the complex of new mutually adjusted results on phase equilibria in the $6\text{Ag}_2\text{X} + \text{Ag}_8\text{B}^{\text{IV}}\text{Te}_6 \leftrightarrow 6\text{Ag}_2\text{Te} + \text{Ag}_8\text{B}^{\text{IV}}\text{X}_6$ reciprocal systems, as well as data on the thermodynamic functions of the Ag_8GeTe_6 compound and $\text{Ag}_8\text{GeSe}_{6-x}\text{Te}_x$ solid solutions, is a contribution to the chemistry, thermodynamics, and materials science of multicomponent chalcogenides. The *practical significance* of the results obtained in the work is, first of all, that the new phases discovered in the studied systems are of great interest as potential thermoelectrics and mixed ion-electron conductive materials. Also, the phase diagrams, crystallographic, thermodynamic, and physicochemical properties of compounds, and phases with variable composition presented in the work are fundamental characteristics of substances and can be included in modern electronic databases and reference books.

According to the international electronic database "Google Scholar Citations", 15 references have been made to the author's articles published on the topic of her dissertation.

Approbation and application of the work. 17 scientific works, including 7 articles (6 articles in journals indexed in the WoS and Scopus databases), have been published on the topic of the dissertation.

The main results of the thesis were discussed at the following conferences: "Müasir təbiət və iqtisad elmlərinin aktual problemləri" beynəlxalq konfrans (Gəncə, Azərbaycan, 2018, 2019, 2020, 2021, 2022, 2023); Rostocker International Conference "Thermophysical Properties for Technical Thermodynamics" (Rostock, Germany, 2020); "Физико-химические процессы в конденсированных средах и на межфазных границах" (Воронеж, Rusiya, 2021);

"Kimyanın müasir problemləri" respublika elmi konfransı (Sumqayıt, Azərbaycan, 2021); XII Международная научная конференция "Кинетика и механизм кристаллизации. Кристаллизация и материалы нового поколения" (Иваново, Россия, 2023).

The results obtained in the dissertation work constitute the scientific basis for the directed synthesis of new solid solution samples discovered in the studied systems and can be used for this purpose. These results can also be used by researchers working in the field of materials science. The results of the work can also be used in teaching specialized courses at the master's degree level of higher educational institutions of the republic.

The name of the organization in which the work was carried out. The dissertation work was performed in the Chemistry Department of the Ganja State University of the Ministry of Science and Education of the Republic of Azerbaijan.

The total volume of the dissertation with a mark, indicates the volume of the structural sections of the dissertation separately. The dissertation consists of an introduction (12045 symbol), five chapters (I chapter 39.963 symbol, II chapter 26.937, III chapter 33.745, IV chapter 22.872, V chapter 22.872), main results, and a list of scientific literature used in 216 titles, and has a volume of 173 pages. The dissertation includes 71 figures and 20 tables.

Acknowledgements. The author expresses deep gratitude to prof. Imameddin Amiraslanov (Institute of Physics) and assoc. Prof. Vagif Gasimov (Institute of Catalysis and Inorganic Chemistry) for their help in conducting X-ray studies.

MAIN CONTENT OF THE WORK

The first chapter of the dissertation provides literature information on phase equilibria in boundary binary and ternary systems of the systems that are the objects of research and on the crystal-chemical, thermal, thermodynamic, etc. properties of intermediate phases. This information was used in planning experimental studies and in developing their results.

Here, literature data on the functional properties of silver

chalcogenides with p²-elements, including the argyrodite family, are also provided, the current state of the physicochemical study of multicomponent chalcogenide systems that form argyrodite-type phases is examined, and the selection of the research objects of the dissertation is justified.

The second chapter provides a brief description of the synthesis methods and reagents used in the work, and briefly explains the methods for obtaining the initial compounds and intermediate alloys of the studied systems.

The synthesis of the initial binary and ternary compounds was carried out by co-melting mixtures of the corresponding simple elements of high purity in stoichiometric ratios in quartz ampoules under vacuum conditions (10⁻²Pa). Since the saturated vapor pressures of sulfur and selenium at the melting temperatures of the compounds are high, the synthesis of sulfides and selenides was carried out in a two-zone mode in an inclined furnace. All synthesized compounds were identified by XRD and DTA methods.

The samples of the studied systems were prepared by co-melting previously synthesized and identified binary and ternary compounds under vacuum conditions. Then, the samples intended for DTA were thermally treated for 500-1000 hours at temperatures 30-500 below the solidus and gradually cooled by disconnecting the furnace from the current source.

In order to construct isothermal sections of the phase diagrams at different temperatures, the samples intended for study by XRD and SEM methods were kept at temperatures corresponding to the corresponding isothermal sections for an additional ~200 hours, and then the ampoules were sharply cooled by dropping them directly from the furnace into ice water.

Information about the research methods used in the work is given in the relevant section in the introduction to the abstract.

Chapter III presents the results of the study of phase equilibria on the 6Ag₂S+Ag₈SiTe₆↔6Ag₂Te+Ag₈SiS₆ and 6Ag₂Se+Ag₈SiTe₆↔Ag₂Te+Ag₈SiSe₆ composition planes of the Ag, Si || S, Te and Ag, Si || Se, Te reciprocal systems [1, 5, 6, 11, 13, 16, 17].

The $6\text{Ag}_2\text{S}+\text{Ag}_8\text{SiTe}_6\leftrightarrow 6\text{Ag}_2\text{Te}+\text{Ag}_8\text{SiS}_6$ system

Powder diffraction patterns of heat-treated and cooled samples of the Ag_8SiS_6 - Ag_8SiTe_6 boundary system of this square are shown in Figure 1. It can be seen from the Figure that the diffraction pattern of the sample containing 10 mol% Ag_8SiTe_6 is similar to the pure Ag_8SiS_6 compound (RT- Ag_8SiS_6) and differs from it only by a small "shift" of the reflection reflexes toward small angles. This is due to an increase in the lattice parameters as a result of the substitution of S-Te. Diffraction patterns of samples containing 30 mol% or more Ag_8SiTe_6 are characteristic of a cubic lattice and are qualitatively similar to the pure Ag_8SiTe_6 compound. The diffraction pattern of the sample containing 20 mol% Ag_8SiTe_6 consists of sets of diffraction lines of primary ternary compounds.

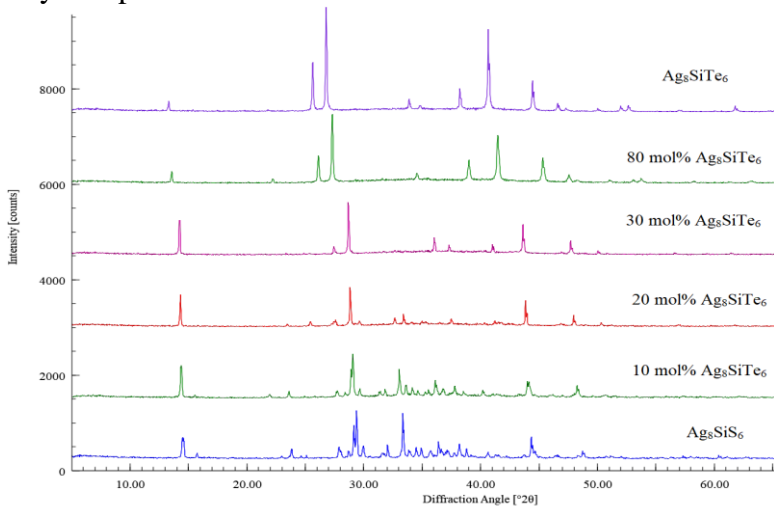


Figure 1. Powder diffractograms of gradually cooled alloys of the Ag_8SiS_6 - Ag_8SiTe_6 system after thermal treatment.

X-ray diffraction phase analysis of samples quenched at 800 K after thermal treatment showed that all samples in the Ag_8SiS_6 - Ag_8SiTe_6 cross-section, including both starting compounds, have a diffraction pattern characteristic of cubic symmetry. This indicates

that at 800 K there is a continuous solid solution order (δ -phase) with a cubic structure between the HT modifications in the system.

The crystal lattice types and parameters of solid solutions at 300 and 800 K were determined by analyzing the powder diffractograms using the TOPAS 3 computer program, and the results are given in Table 1.

Figure 2 shows the phase diagram of the Ag_8SiS_6 - Ag_8SiTe_6 system. As can be seen, the system is quasi-binary and forms a continuous solid solution sequence (δ -phase) between HT- Ag_8SiS_6 and Ag_8SiTe_6 compounds. The formation of the δ -phase is accompanied by a sharp decrease in the polymorphic transformation temperature of the Ag_8SiS_6 compound and a transition from room temperature to a region below the temperature of about 25 mol% Ag_8SiTe_6 .

Table 1
Crystal lattice types and parameters of compounds and solid solutions of the Ag_8SiS_6 - Ag_8SiTe_6 system

Composition, mol% Ag_8SiTe_6	Singony, Sp.gr, crystal lattice parameters, nm	
	Room temperature	Quenched from 800 K temperature
0 (Ag_8SiS_6)	orthorhombic, Pna2 ₁ , $a=1.5032(3)$, $b=0.7430(2)$, $c=1.0538(3)$	cunib, F43m, $a=1.0635(3)$
10	orthorhombic, Pna2 ₁ , $a=1.5146(4)$; $b=0.749(3)$; $c=1.0627(3)$	"-, $a=1.0733(3)$
20	Two-phase $\gamma+\delta$	"-, $a=1.0824(4)$
30	cubik, F43m, $a=1.0906(3)$	"-, $a=1.0915(4)$
40	"-, $a=1.0995(3)$	"-, $a=1.1002(3)$
60	"-, $a=1.1162(4)$	"-, $a=1.1167(4)$
80	"-, $a=1.1335(4)$	"-, $a=1.1344(3)$
Ag_8SiTe_6	"-, $a=1.1524(4)$	"-, $a=1.1528(3)$

It can be seen from Figure 2 that the cubic lattice of both the samples quenched at 800 K and the samples with ≥ 30 mol% Ag_8SiTe_6 content slowly cooled after thermal treatment is a linear

function of the periodic composition, i.e., the solid solutions satisfy Vegard's rule.

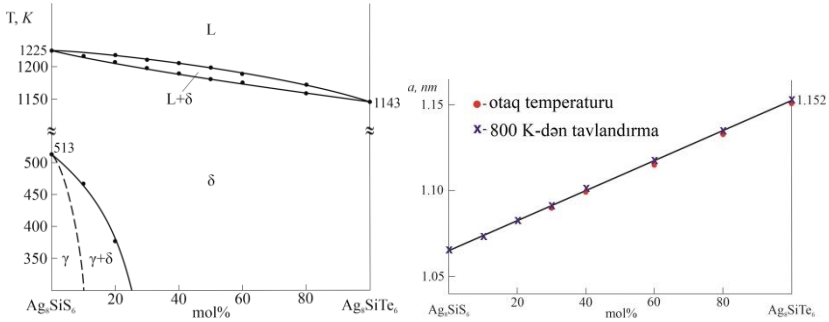


Figure 2. Phase diagram of the $\text{Ag}_8\text{SiS}_6\text{-Ag}_8\text{SiTe}_6$ system and dependence of lattice parameters on the composition

Figure 3 shows the solid-phase equilibria of the reciprocal system at 800 and 300 K.

The isothermal section at 800 K represents a relatively simple phase equilibria. At this temperature, wide regions of α - and β' -solid solutions existing at the $\text{Ag}_2\text{S-Ag}_2\text{Te}$ boundary system are in equilibrium with δ -solid solutions of the $\text{Ag}_8\text{SiS}_6\text{-Ag}_8\text{SiTe}_6$ boundary system and forming $\alpha+\delta$, $\alpha+\beta'$, $\beta'+\delta$ two-phase and $\alpha+\beta'+\delta$ three-phase fields.

The isothermal section at 300 K. At this temperature, in the $\text{Ag}_2\text{S-Ag}_2\text{Te}$ boundary system, along with the Ag_4TeS compound (ϵ -phase), there are 5-10 mol% solid solutions (α' - and β'' -phases) based on low-temperature modifications of the initial compounds. On the other hand, according to the phase diagram constructed by us, in the $\text{Ag}_8\text{SiS}_6\text{-Ag}_8\text{SiTe}_6$ system (Fig. 2), there are ~10 mol% solid solutions (γ -phase) based on RT- Ag_8SiS_6 , and ~75 mol% solid solutions (δ -phase) based on Ag_8SiTe_6 . These fields form a series of two-phase ($\alpha'+\gamma$, $\alpha'+\epsilon$, $\gamma+\epsilon$, $\beta''+\epsilon$, $\beta''+\delta$, $\beta'+\epsilon$) and three-phase ($\alpha'+\gamma+\epsilon$, $\beta''+\gamma+\epsilon$ və $\beta''+\gamma+\delta$) fields with each other.

The projection of the liquidus surface (Fig. 4) consists of the initial crystallization area of the three phases. They are bounded by monovariant equilibrium curves and the triple eutectic point. The

types and temperatures of non- and monovariant equilibria are given in Table 2.

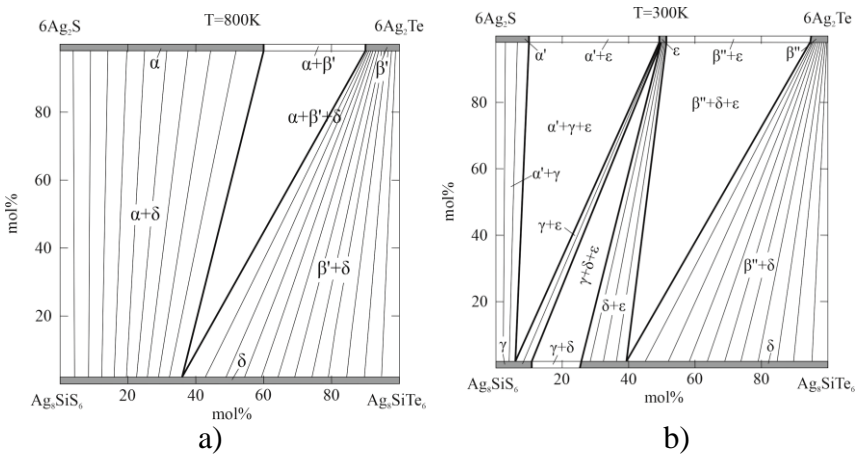


Figure 3. Isothermal sections of the phase diagram of the $\text{Ag}_2\text{S} + \text{Ag}_8\text{SiTe}_6 \leftrightarrow 6\text{Ag}_2\text{Te} + \text{Ag}_8\text{SiS}_6$ reciprocal system at 800 K (a) and 300 K (b)

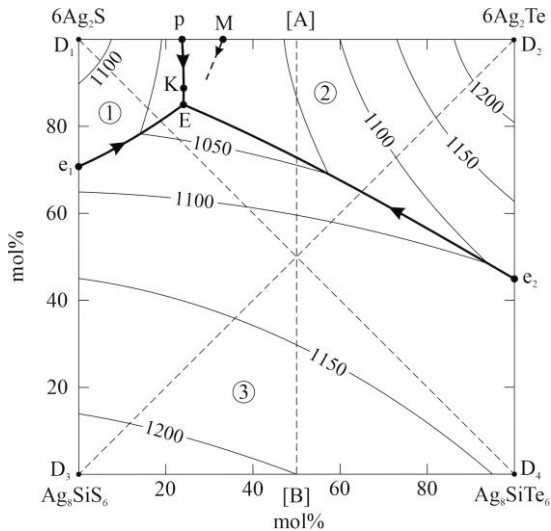


Figure 4. Projection of the liquidus surface of the $6\text{Ag}_2\text{S} + \text{Ag}_8\text{SiTe}_6 \leftrightarrow 6\text{Ag}_2\text{Te} + \text{Ag}_8\text{SiS}_6$ system. Primary crystallization areas: 1- α' ; 2- α ; 3- δ ; 4- β'

A characteristic feature of this reciprocal system is that three of the four initial compounds have polymorphic phase transitions. These phase transitions seriously affect the nature of the phase equilibria in the subsolidus region of the system and complicate it. In order to reflect the processes occurring in the subsolidus in more detail, some polythermal and isothermal sections of the phase diagram of the system are given and discussed in detail in the dissertation work.

Table 2
Non- and monovariant equilibria in the reciprocal system $6\text{Ag}_2\text{S}+\text{Ag}_8\text{SiTe}_6\leftrightarrow 6\text{Ag}_2\text{Te}+\text{Ag}_8\text{SiS}_6$

Point or curve in Fig.4	Equilibria	T, K
D ₁	$L \leftrightarrow \text{HT-Ag}_2\text{S} (\alpha^*)$	1110
D ₂	$L \leftrightarrow \text{HT-Ag}_2\text{Te} (\beta^1)$	1238
D ₃	$L \leftrightarrow \text{HT-Ag}_8\text{SiS}_6 (\delta)$	1230
D ₄	$L \leftrightarrow \text{Ag}_8\text{SiTe}_6 (\delta)$	1143
P	$L + \alpha^* \leftrightarrow \alpha$	1033
M	$L \leftrightarrow \alpha$	1025
K	Transition point	1010
e ₁	$L \leftrightarrow \alpha^1 (\alpha) + \delta$	1085
e ₂	$L \leftrightarrow \alpha + \delta$	1105
E	$L \leftrightarrow \alpha + \alpha^* + \delta$	1015
PK	$L + \alpha^* \leftrightarrow \alpha$	1033-1020
KE	$L \leftrightarrow \alpha^* + \alpha$	1020-1015
e ₁ E	$L \leftrightarrow \alpha^* + \delta$	1010-980
e ₂ E	$L \leftrightarrow \alpha + \delta$	1105-960

Note: Here, in the phase diagrams and the text, the phase designations are: α^* – (HT-Ag₂S); α – are continuous solid solutions between IT-Ag₂S and HT-Ag₂Te; β^1 – (IT-Ag₂Te); δ – are continuous solid solutions between HT-Ag₈SiS₆ and Ag₈SiTe₆

The $6\text{Ag}_2\text{Se}+\text{Ag}_8\text{SiTe}_6\leftrightarrow 6\text{Ag}_2\text{Te}+\text{Ag}_8\text{SiSe}_6$ reciprocal system

The XRD results of the slowly cooled samples from the thermal treatment on the Ag₈SiSe₆-Ag₈SiTe₆ boundary system of this system (Fig. 5) show that the samples with 10-90 mol% Ag₈SiTe₆ content have a diffraction pattern characteristic of cubic symmetry

belonging to the $F-43m$ Space group and are qualitatively identical to the powder diffractogram of the Ag_8SiTe_6 compound. Even in the sample with 10 mol% Ag_8SiTe_6 content, the low-temperature diffraction lines of the Ag_8SiSe_6 compound are not observed.

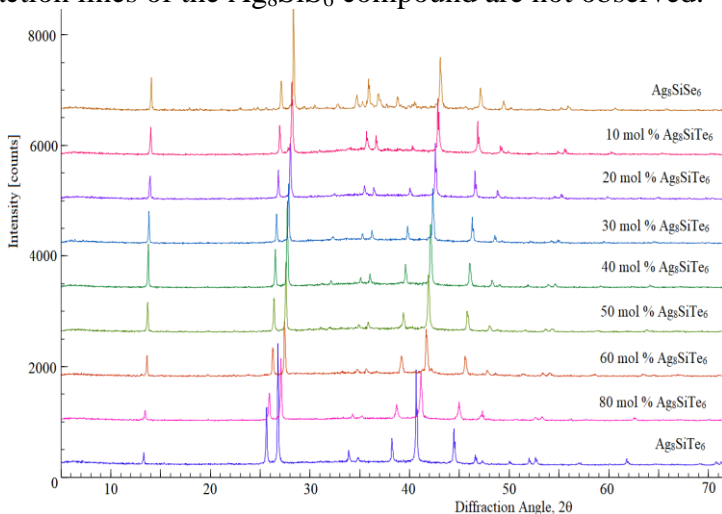


Figure 5. Powder diffractograms of some alloys of the Ag_8SiSe_6 - Ag_8SiTe_6 system

Analysis of this picture leads to the conclusion that a continuous series of solid solutions are formed in the system based on high-temperature cubic modifications of the initial compounds, and at this time the temperatures of polymorphic transition of the Ag_8SiSe_6 compound (354 and 313 K) decrease sharply.

The results of X-ray diffraction analysis of samples quenched from 800 K showed that their diffractograms also have diffraction lines characteristic of cubic syngony and a slight shift of the diffraction lines towards small angles occurs. This can be explained by the thermal expansion of the crystal lattice.

The phase diagram of the Ag_8SiSe_6 - Ag_8SiTe_6 system (Figure 6) fully confirms the XRD results.

As can be seen, the phase diagram does not show any effects related to the polymorphic transformation of the Ag_8SiSe_6 compound. This indicates that the formation of solid solutions sharply re-

duces the transformation temperatures and they are no longer observed in the DTA curves at 10 mol% Ag_8SiTe_6 .

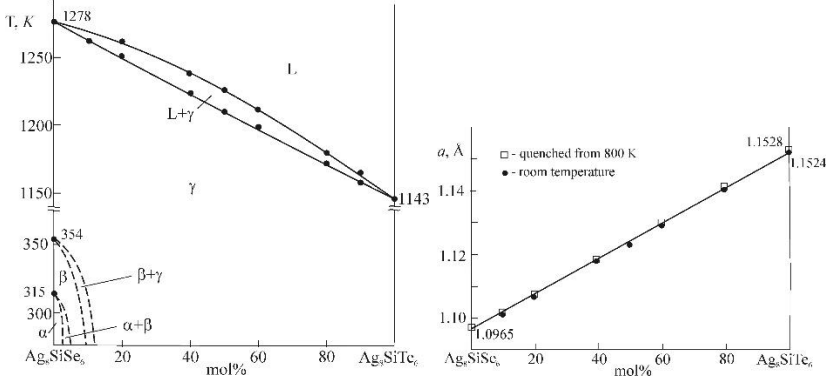


Figure 6. Phase diagram of the Ag_8SiSe_6 - Ag_8SiTe_6 system and dependence of the lattice period of solid solutions on composition

The composition dependences of the lattice periods of both slowly cooled and quenched solid solution samples obey Vegard's rule (Fig. 6).

The projection of the liquidus surface consists of two wide areas of the primary crystallization phases (Fig. 7). They represent the primary crystallization of continuous high-temperature solid solutions (α -phase) at the Ag_2Se - Ag_2Te boundary system and the primary crystallization of high-temperature solid solutions (δ -phase) at the $\text{Ag}_8\text{SiTe}_6 \leftrightarrow \text{Ag}_8\text{SiSe}_6$ boundary system. These surfaces are limited by the $L \leftrightarrow \alpha + \delta$ monovariant eutectic equilibrium curve (e_1e_2).

The data collected in Figure 7 allows tracking of the crystallization processes of a liquid solution of any composition in the system. However, the fact that the primary compounds have polymorphic transformations leads to a complex nature of phase equilibria in the subsolidus part of the reciprocal system. For a detailed study of the processes associated with phase transformations, several polythermal sections of the phase diagram are presented and described in the dissertation.

Chapter IV presents the results of the study of phase

equilibria in the $6\text{Ag}_2\text{S}+\text{Ag}_8\text{GeTe}_6\leftrightarrow 6\text{Ag}_2\text{Te}+\text{Ag}_8\text{GeS}_6$ and $6\text{Ag}_2\text{Se}+\text{Ag}_8\text{GeTe}_6\leftrightarrow \text{Ag}_2\text{Te}+\text{Ag}_8\text{GeSe}_6$ composition planes of the Ag, Ge || S, Te and Ag, Ge || Se, Te reciprocal systems [2,3,7.8,9,13,15].

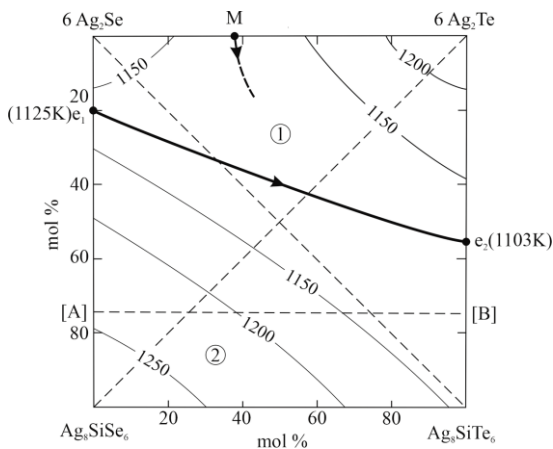


Figure 7. Projection of the liquidus surface of the $6\text{Ag}_2\text{Se}+\text{Ag}_8\text{SiTe}_6\leftrightarrow 6\text{Ag}_2\text{Te}+\text{Ag}_8\text{SiSe}_6$ system. Primary crystallization regions: 1- α ; 2- δ .

Our studies have shown that, as in the corresponding silicon systems, continuous cubic solid solution series are formed in these systems in the Ag_8GeS_6 - Ag_8GeTe_6 and Ag_8GeSe_6 - Ag_8GeTe_6 boundary systems. However, there are limited solubility regions based on low-temperature modifications of sulfide and selenide compounds (Fig. 8).

Unlike the corresponding silicon systems (Fig. 1 and 6), these systems are only partially quasi-binary. This is because one of their initial components, the Ag_8GeTe_6 compound, melts incongruently. Therefore, in the Ag_8GeTe_6 -rich region of both systems, not δ -solid solutions, but solid solutions (β') based on IT- Ag_2Te initially crystallize from the liquid phase. After the initial crystallization of this phase, monovariant co-crystallization of the β' and δ -phases occurs, and the $L+\beta'+\delta$ three-phase region is formed in the

systems. The eutectic process ends with the complete consumption of the β' -phase, and crystallization in subsequent stages proceeds according to the $L \leftrightarrow \delta$ scheme.

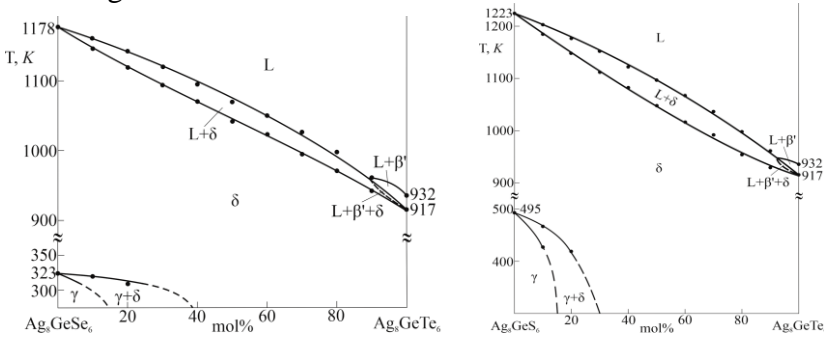


Figure 8. Phase diagrams of the $\text{Ag}_8\text{GeSe}_6\text{-Ag}_8\text{GeTe}_6$ and $\text{Ag}_8\text{GeS}_6\text{-Ag}_8\text{GeTe}_6$ systems

It should be noted that the formation of solid solutions in the $\text{Ag}_8\text{GeSe}_6\text{-Ag}_8\text{GeTe}_6$ and $\text{Ag}_8\text{GeS}_6\text{-Ag}_8\text{GeTe}_6$ systems leads to a sharp decrease in the polymorphic transformation temperature of the initial sulfide and selenide compounds and an expansion of the continuum region of the cubic high-temperature phases to room temperature and below.

The phase equilibria on isothermal sections at 300 K are similar in nature to the corresponding silicon systems and differ from them in the coordinates of the phase fields (Fig. 9).

In the dissertation work, a projection of the liquidus surface of the $6\text{Ag}_2\text{Se} + \text{Ag}_8\text{GeTe}_6 \leftrightarrow \text{Ag}_2\text{Te} + \text{Ag}_8\text{GeSe}_6$ reciprocal system was constructed (Figure 10). The liquidus surface consists of two large areas reflecting the initial crystallization of continuous high-temperature solid solutions (α -phase) in the $\text{Ag}_2\text{Se-Ag}_2\text{Te}$ boundary system and high-temperature solid solutions (δ -phase) formed in the $\text{Ag}_8\text{GeSe}_6\text{-Ag}_8\text{GeTe}_6$ boundary system and a third small area related to solid solutions (β' -phase) based on $\text{IT-Ag}_2\text{Te}$. The liquidus surfaces of the α - and δ -phases are limited by a eutectic curve emanating from the point e (1100 K) in a wide interval and reflect

ting the $L \leftrightarrow \alpha + \delta$ monovariant equilibrium. This curve intersects with the curve emanating from the point P_1 (1063 K) at point U (950 K), and creates a nonvariant transition equilibrium:

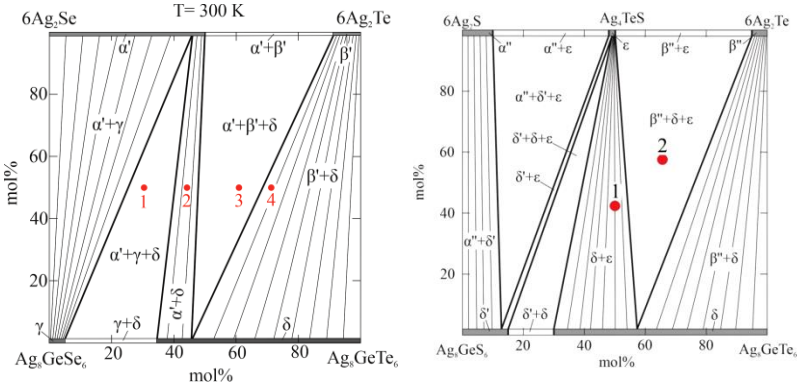


Figure 9. Isothermal sections of the phase diagrams of the $6Ag_2S+Ag_8GeTe_6 \leftrightarrow 6Ag_2Te+Ag_8GeSe_6$ and $6Ag_2Se+Ag_8GeTe_6 \leftrightarrow 6Ag_2Te+Ag_8GeSe_6$ reciprocal systems at 300 K

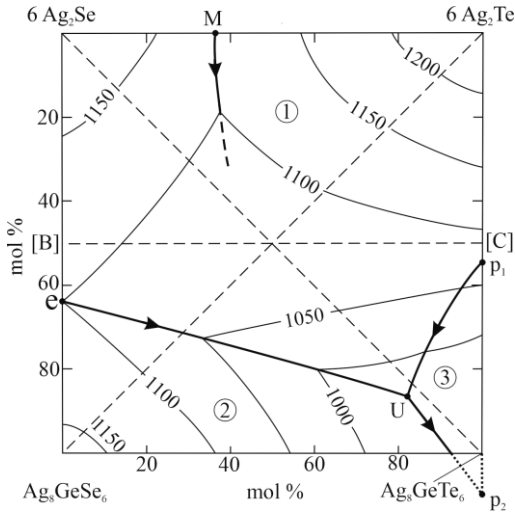
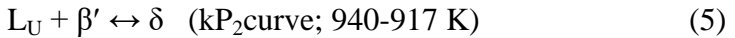
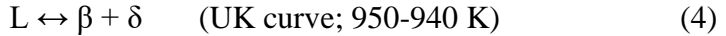
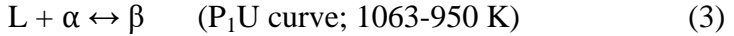
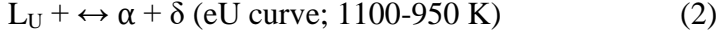


Figure 10. Projection of the liquidus surface of the $6Ag_2Se+Ag_8GeTe_6 \leftrightarrow 6Ag_2Te+Ag_8GeSe_6$ reciprocal system. Primary crystallization regions: 1- α ; 2- δ ; 3- β



At the beginning of the UP₂ curve (UK) emanating from point U, there is a monovariant eutectic equilibrium $L \leftrightarrow \beta' + \delta$. In the part of the curve outside the compositions square (kP₂), this equilibrium turns into a peritectic equilibrium.

Thus, the following monovariant equilibria exist in the reciprocal system:



In the Ag₂Se-Ag₂Te boundary system, leaving the minimum point (M), reflecting the invariant equilibrium $L \leftrightarrow \alpha$, the monovariant equilibrium curve disappears within the square, and the liquidus surface of the α -phase becomes a homogeneous surface (Fig. 10).

For a more detailed analysis of the crystallization processes and transformations occurring in the subsolidus, a number of polythermal and high-temperature isothermal sections of the phase diagram of the $6\text{Ag}_2\text{Se} + \text{Ag}_8\text{GeTe}_6 \leftrightarrow 6\text{Ag}_2\text{Te} + \text{Ag}_8\text{GeSe}_6$ reciprocal system are constructed and discussed in the dissertation. Some of them are given below.

6Ag₂Se-Ag₈GeTe₆ polythermal cross section (Fig. 11). On this cross-section, the liquidus consists of two curves corresponding to the initial crystallization of the α - and β -phases. These curves intersect at ~85 mol% Ag₈GeTe₆ composition. Below the liquidus, in the ~3-70 mol% Ag₈GeTe₆ composition interval, crystallization continues according to the monovariant eutectic reaction (2) (Fig. 10, eU-curve). During this process, a three-phase $L + \alpha + \delta$ region is formed on the T-x diagram. In a wide (~3-60 mol% Ag₈GeTe₆) composition interval, crystallization ends with reaction (2), and an $\alpha + \delta$ two-phase region is formed in the subsolidus. After crystallization of the β -phase from the liquid solution in the 80-100 mol% Ag₈GeTe₆ composition interval, the eutectic reaction $L \leftrightarrow \beta + \delta$ (4) begins, and upon its completion, a $\beta + \delta$ two-phase mixture is obtained. The horizontal line (1) corresponding to 950 K reflects the

nonvariant transition reaction. When this reaction ends with the excess of the liquid phase, the system passes into the $L+\beta+\delta$ three-phase state (in the range of >75 mol% Ag_8GeTe_6 composition), the liquid phase is completely consumed in the reaction, and when a part of the α -phase remains in excess (~ 60 - 75 mol% Ag_8GeTe_6), an $\alpha+\beta+\delta$ three-phase mixture is obtained.

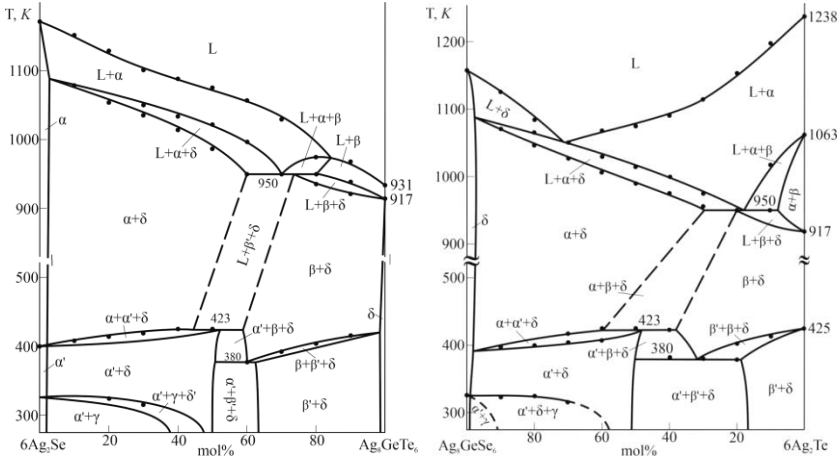


Figure 11. $6\text{Ag}_2\text{Se}-\text{Ag}_8\text{GeTe}_6$ and $\text{Ag}_8\text{GeSe}_6-6\text{Ag}_2\text{Te}$ polythermal sections of the phase diagram

In a wide temperature range (917-423 K) the system retains the $\alpha+\delta$, $\alpha+\beta+\delta$, $\beta+\delta$ heterogeneous regions. The formation of solid solutions based on the Ag_2S compound increases its polymorphic transformation temperature (from ~ 400 K to 423 K), while solutions based on the Ag_2Te and Ag_8GeTe_6 compounds reduce their phase transition temperatures (Fig. 11).

The horizontal lines at 423 and 380 K correspond to the $\alpha+\beta \leftrightarrow \alpha'+\delta$ peritectoid and $\beta \leftrightarrow \alpha'+\beta'+\delta$ eutectoid equilibria, respectively. The decrease in the structural transformation ($\delta \leftrightarrow \gamma$) temperature in solid solutions based on the Ag_8GeSe_6 compounds can most likely lead to the formation of the $\delta \leftrightarrow \alpha'+\beta'+\gamma$ eutectoid equilibrium, which is much lower than room temperature.

$\text{Ag}_8\text{GeSe}_6-6\text{Ag}_2\text{Te}$ polythermal cross section (Fig. 11). This

cross-section passes through the liquidus surfaces of the α - and δ -phases. At the intersection of the liquidus curves (~ 70 mol% Ag_8GeSe_6 , 1050 K), an $\alpha+\delta$ eutectic mixture crystallizes from the liquidus by reaction (2). Below the liquidus, this monovariant process occurs over a wide concentration range (20-98 mol% Ag_8GeSe_6), and an $\alpha+\delta$ two-phase region formed in the phase diagram.

After the initial crystallization of the α -phase in the Ag_2Te -rich region (0-20 mol% Ag_8GeSe_6), the $L+\alpha\leftrightarrow\beta$ peritectoid reaction (p_1U -curve in Fig. 10) begins in the system and the $L+\alpha+\beta$ three-phase region is formed. When the crystallization is completed by this reaction, the $\alpha+\beta$ two-phase region is formed in the system. The horizontal line at 950 K, as in the polythermal section considered above, reflects the nonvariant transition reaction (1). This reaction ends with the formation of a $\beta+\delta$ mixture in the composition of ~ 20 mol% Ag_8GeSe_6 . Depending on whether this reaction ends in a liquid or α -phase deficiency, $\alpha+\beta+\delta$ or $\beta+\delta$ heterogeneous regions are formed in the subsolidus.

Isothermal sections of the phase diagram at 1100 and 1000 K.

In the dissertation work, along with the isothermal sections of the phase diagram of the $6\text{Ag}_2\text{Se}+\text{Ag}_8\text{GeTe}_6\leftrightarrow 6\text{Ag}_2\text{Te}+\text{Ag}_8\text{GeSe}_6$ reciprocal system at 300 and 800 K, the isothermal sections of the phase diagram at higher (1100 and 1000 K) temperatures were constructed. These diagrams reflect the “liquid \leftrightarrow crystal” equilibria in the system and are interesting from the point of view of growing monocrystals by direct crystallization.

The isothermal section at 1100 K (Fig. 12) reflects the equilibrium regions of the liquid phase with the α - and δ -phases, the composition of which varies in a certain interval. The unconventional shape of the isotherm delimiting the $L+\alpha$ two-phase region is due to the influence of the curve emanating from the M-minimum point (Fig. 10). By choosing the composition of the solid phase on the connode lines (the δ -phase corresponding to point "s" in Figure 12), the composition of the liquid phase in equilibrium with it (the point "l" in the connode connection with point "s") can be determined. It is clear that by directional crystallization of the liquid phase

with composition "l" single crystals of the δ -phase with composition "s" can be grown.

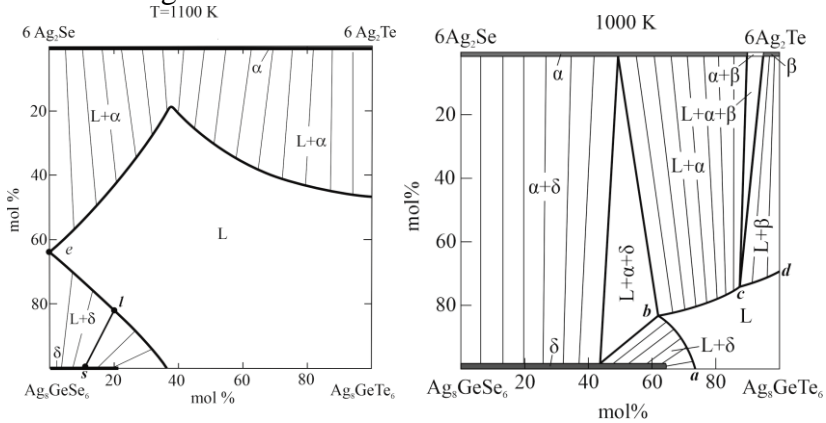


Figure 12. Isothermal sections of the phase diagram at 1100 and 1000 K

The isothermal section at 1100 K (Figure 12). It can be seen that at this temperature the liquid phase in the system is in equilibrium with the α -phase (bc -curve) whose composition varies over a wide range (~ 50 - 90 mol% Ag_2Te), with the β -phase in the range of 95 - 100 mol% Ag_2Te (cd -curve), and with the δ -phase (ab -curve) whose composition covers the range of 45 - 65 mol% Ag_8GeTe_6 . Therefore, this isothermal section can be used to obtain single crystals of these phases with a given composition by directional crystallization.

In the areas rich in Ag_2Se and Ag_8SiSe_6 only crystalline phases participate in the phase equilibria.

Thus, the considered polythermal and isothermal sections clearly reflect the processes of crystallization from the liquid in the reciprocal system and the processes associated with phase transformations in the subsolidus. They are in full agreement both with each other and with the solid-phase equilibria diagrams at 300 and 800 K as well as with the projection of the liquidus surface of the reciprocal system.

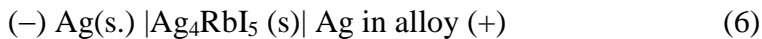
Chapter V is devoted to the investigations of the thermodyna-

mic properties of some three- and four-component phases formed in the systems studied in the dissertation work by the electromotive force (EMF) method [4,10,12].

At the beginning of the chapter (paragraphs 5.1 and 5.2.) the basics of the EMF method are briefly explained and the features of the application of this method to multicomponent multiphase heterogeneous systems are examined. It also provides information (paragraph 5.3.) about the EMF method using solid electrolyte and its application to inorganic systems. In the following sections of the chapter, methodological issues of studies using the EMF method and methods for mathematical processing of the results are given (paragraphs 5.4 and 5.5). In the last two paragraphs, the results of the thermodynamic study of the Ag_8GeTe_6 compound and $\text{Ag}_8\text{GeTe}_{6-x}\text{Se}_x$ solid solutions are presented and discussed.

Thermodynamic properties of the Ag_8GeTe_6 compound and $\text{Ag}_8\text{GeTe}_{6-x}\text{Se}_x$ solid solutions.

To conduct thermodynamic studies, the



type concentration cells were assembled. In these cells, the Ag_4RbI_5 compound with pure Ag^+ cation conductivity was used as a solid electrolyte. EMF measurements were carried out in the temperature range of 300-400 K using a Keithley 2100 6 ½ high-resistance multimeter.

Figure 11 shows the temperature dependencies of the EMF values obtained for the Ag_8GeTe_6 compound and various compositions of the $\text{Ag}_8\text{GeTe}_{6-x}\text{Se}_x$ solid solutions. As can be seen, the temperature dependences of the EMF for all samples are linear within the error. Therefore, the results of the measurements were processed using a special computer program by the least squares method and the method recommended in modern scientific literature⁵

⁵ Морачевский А.Г., Воронин Г.Ф., Гейдерих В.А. Электрохимические методы исследования в термодинамике металлических систем. Москва: ИЦК «Академкнига», - 2003. - 334 с.

$$E = a + bT \pm t \left[(S_E^2 / n) + S_b^2 \cdot (T - \bar{T})^2 \right]^{1/2} \quad (7)$$

and linear equations of the type (5) were obtained. In equation (7), n —number of pairs of E and T values; S_E and S_b —respectively, the variance of individual EMF measurements and the b coefficient; \bar{T} — average temperature, K; t —Student criterion. At the 95% confidence level, when $n \geq 30$, $t \leq 2$.

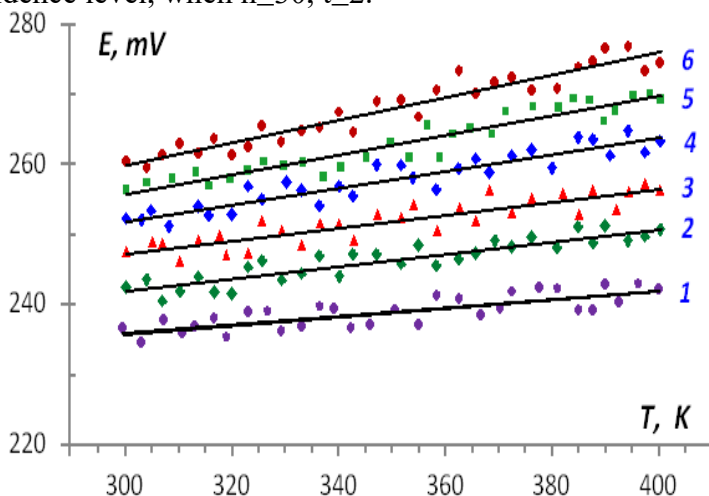


Figure 11. Temperature dependences of EMF values for argyrodite phases with different compositions in the temperature range of 300–400 K. 1- Ag_8GeTe_6 ; 2- $\text{Ag}_8\text{GeTe}_5\text{Se}$; 3- $\text{Ag}_8\text{GeTe}_4\text{Se}_2$; 4- $\text{Ag}_8\text{GeTe}_3\text{Se}_3$; 5- $\text{Ag}_8\text{GeTe}_2\text{Se}_4$; 6- $\text{Ag}_8\text{GeTeSe}_5$.

Linear equations of type (7) obtained for the Ag_8GeTe_6 compound and various compositions of the $\text{Ag}_8\text{GeTe}_{6-x}\text{Se}_x$ solid solutions are given in Table 3. Based on these equations, the partial molar Gibbs free energy, enthalpy, and entropy of silver in these phases, as well as the errors of these quantities, were calculated based on known thermodynamic expressions (Table 4). The quantities given in this Table are thermodynamic functions of certain potential forming reactions, and the equations of these reactions were used to calculate the integral thermodynamic functions of these compounds and phases. For this purpose, the phase diagrams of the corresponding systems were used.

Table 3

Temperature dependences of the EMF of the concentration cells of type (7) for alloys of the Ag_8GeSe_6 - Ag_8GeTe_6 system (T=300-400 K)

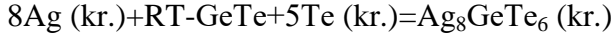
Phase	$E, \text{mV} = a + bT \pm 2\tilde{S}_E(T)$
Ag_8GeTe_6	$217.59 + 0.0608T \pm 2 \left[\frac{2.02}{30} + 7.3 \cdot 10^{-5}(T-349.8)^2 \right]^{1/2}$
$\text{Ag}_8\text{GeTe}_5\text{Se}$	$214.87 + 0.0896T \pm 2 \left[\frac{1.62}{30} + 5.8 \cdot 10^{-5}(T-350.0)^2 \right]^{1/2}$
$\text{Ag}_8\text{GeTe}_4\text{Se}_2$	$213.53 + 0.1120T \pm 2 \left[\frac{1.80}{30} + 6.5 \cdot 10^{-5}(T-350.1)^2 \right]^{1/2}$
$\text{Ag}_8\text{GeTe}_3\text{Se}_3$	$216.29 + 0.1186T \pm 2 \left[\frac{2.01}{30} + 7.2 \cdot 10^{-5}(T-349.7)^2 \right]^{1/2}$
$\text{Ag}_8\text{GeTe}_2\text{Se}_4$	$213.54 + 0.1404T \pm 2 \left[\frac{1.92}{30} + 7.0 \cdot 10^{-5}(T-352.9)^2 \right]^{1/2}$
$\text{Ag}_8\text{GeTeSe}_5$	$211.24 + 0.1617T \pm 2 \left[\frac{2.14}{30} + 7.7 \cdot 10^{-5}(T-350.0)^2 \right]^{1/2}$

Table 4

Partial molar functions of silver in alloys of the Ag_8GeSe_6 - Ag_8GeTe_6 system at 298 K

Phase	$-\Delta\bar{G}_{\text{Ag}}$	$-\Delta\bar{H}_{\text{Ag}}$	$\Delta\bar{S}_{\text{Ag}},$
	$\text{kJ} \cdot \text{mol}^{-1}$		$\text{J} \cdot \text{K}^{-1} \cdot \text{mol}^{-1}$
Ag_8GeTe_6	22.74 ± 0.05	21.00 ± 0.29	5.84 ± 0.82
$\text{Ag}_8\text{GeTe}_5\text{Se}$	23.31 ± 0.04	20.73 ± 0.26	8.64 ± 0.74
$\text{Ag}_8\text{GeTe}_4\text{Se}_2$	23.83 ± 0.05	20.60 ± 0.27	10.81 ± 0.78
$\text{Ag}_8\text{GeTe}_3\text{Se}_3$	24.28 ± 0.05	20.87 ± 0.29	11.44 ± 0.82
$\text{Ag}_8\text{GeTe}_2\text{Se}_4$	24.64 ± 0.05	20.60 ± 0.29	13.54 ± 0.81
$\text{Ag}_8\text{GeTeSe}_5$	25.04 ± 0.05	20.38 ± 0.30	15.61 ± 0.85

In the Ag-Ge-Te system, the Ag_8GeTe_6 compound is in three-phase equilibrium with GeTe and elemental tellurium. Therefore, the potentialforming reaction for this ternary compound corresponds to the relation.



According to this equation, the standard Gibbs free energy and enthalpy of formation of that compound was calculated using the equation

$$\Delta_f Z^0(\text{Ag}_8\text{GeTe}_6) = 8\Delta\bar{Z}_{\text{Ag}} + \Delta_f Z^0(\text{GeTe}) \quad (8)$$

Here $Z \equiv G, H$.

The standard entropy was calculated using the relation

$$S^0(\text{Ag}_8\text{GeTe}_6) = 8[\Delta\bar{S}_{\text{Ag}} + S^0(\text{Ag})] + 5S^0(\text{Te}) + S^0(\text{GeTe}) \quad (9)$$

From the schematic solid-state equilibria diagram of the Ag-Ge-Se-Te system (Fig. 12) it can be seen that on the 2-2' rays in the solid tetrahedron, the alloys are in the $\text{Ag}_8\text{GeTe}_5\text{Se} + \text{GeTe} + \text{GeSe}_2 + \text{Te}$ four-phase state, and on the 3-3' ray line they are in the $\text{Ag}_8\text{GeTe}_4\text{Se}_2 + \text{GeSe}_2 + \text{Te}$ three-phase state. On the other hand, on the 4-4', 5-5' and 6-6' ray lines, the alloys are also in the $\delta + \text{GeSe}_2 + \alpha$ three-phase state.

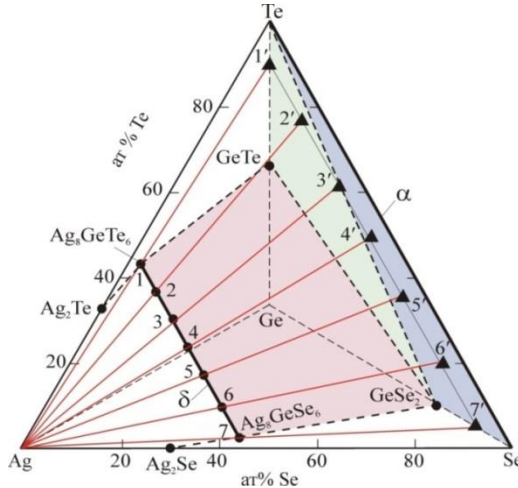
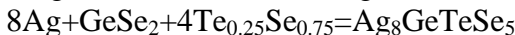
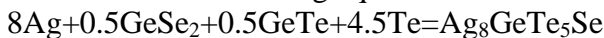


Figure 12. Fragment of the solid-state equilibria diagram of the Ag-Ge-Se-Te system at room temperature. The colored planes are the phase planes $\text{GeSe}_2\text{-Te-Se}$ (blue), $\text{GeSe}_2\text{-GeTe-Te}$ (green), $\text{Ag}_8\text{GeTe}_6\text{-Ag}_8\text{GeSe}_6\text{-GeSe}_2\text{-GeTe}$ (pink). The red straight lines are the ray lines emanating from the Ag vertex of the solid tetrahedron and passing through the different compositions of the $\text{Ag}_8\text{GeTe}_{6-x}\text{Se}_x$ solid solutions.

The above phase compositions of the alloys show that the potential-forming reactions for δ -solid solutions of various compositions are in the form of the following equations:



According to these equations, the standard thermodynamic functions of formation for the above-mentioned compositions of solid solutions are

$$\Delta_f Z^0(\text{Ag}_8\text{GeTe}_5\text{Se}) = 8\Delta\bar{Z}_{\text{Ag}} + 0.5\Delta_f Z^0(\text{GeSe}_2) + 0.5\Delta_f Z^0(\text{GeTe})$$

$$\Delta_f Z^0(\text{Ag}_8\text{GeTe}_4\text{Se}_2) = 8\Delta\bar{Z}_{\text{Ag}} + \Delta_f Z^0(\text{GeSe}_2)$$

$$\Delta_f Z^0(\text{Ag}_8\text{GeTe}_3\text{Se}_3) = 8\Delta\bar{Z}_{\text{Ag}} + \Delta_f Z^0(\text{GeSe}_2) + 4\Delta_f Z^0(\text{Te}_{0.75}\text{Se}_{0.25})$$

$$\Delta_f Z^0(\text{Ag}_8\text{GeTe}_2\text{Se}_4) = 8\Delta\bar{Z}_{\text{Ag}} + \Delta_f Z^0(\text{GeSe}_2) + 4\Delta_f Z^0(\text{Te}_{0.5}\text{Se}_{0.5})$$

$$\Delta_f Z^0(\text{Ag}_8\text{GeSe}_5\text{Te}) = 8\Delta\bar{Z}_{\text{Ag}} + \Delta_f Z^0(\text{GeSe}_2) + 4\Delta_f Z^0(\text{Te}_{0.25}\text{Se}_{0.75})$$

While standard entropy is calculated based on the relations

$$S^0(\text{Ag}_8\text{GeTe}_5\text{Se}) = 8\Delta\bar{S}_{\text{Ag}} + 8S^0(\text{Ag}) + 4.5S^0(\text{Te}) + S^0(\text{GeSe}_2) + 0.5S^0(\text{GeTe})$$

$$S^0(\text{Ag}_8\text{GeTe}_4\text{Se}_2) = 8\Delta\bar{S}_{\text{Ag}} + 8S^0(\text{Ag}) + 4S^0(\text{Te}) + S^0(\text{GeSe}_2)$$

$$S^0(\text{Ag}_8\text{GeTe}_3\text{Se}_3) = 8\Delta\bar{S}_{\text{Ag}} + 8S^0(\text{Ag}) + S^0(\text{GeSe}_2) + 4S^0(\text{Te}_{0.75}\text{Se}_{0.25})$$

$$S^0(\text{Ag}_8\text{GeTe}_2\text{Se}_4) = 8\Delta\bar{S}_{\text{Ag}} + 8S^0(\text{Ag}) + S^0(\text{GeSe}_2) + 4S^0(\text{Te}_{0.5}\text{Se}_{0.5})$$

$$S^0(\text{Ag}_8\text{GeSe}_5\text{Te}) = 8\Delta\bar{S}_{\text{Ag}} + 8S^0(\text{Ag}) + S^0(\text{GeSe}_2) + 4S^0(\text{Te}_{0.25}\text{Se}_{0.75})$$

The standard integral thermodynamic functions obtained for the Ag_8GeTe_6 compound and $\text{Ag}_8\text{GeTe}_{6-x}\text{Se}_x$ solid solutions as a result of the calculations are given in Table 5. The thermodynamic quantities recommended in modern databases were used in the calculations. The following values were used for the absolute entropies of the elementary components:

$$S^0(\text{Ag}) = 42.55 \pm 0.13 \text{ J}\cdot\text{mol}^{-1}\cdot\text{K}^{-1}; S^0(\text{Te}) = 49,50 \pm 0,21 \text{ J}\cdot\text{mol}^{-1}\cdot\text{K}^{-1}$$

The standard integral thermodynamic functions used in the calculations for the GeTe and GeSe₂ compounds used in the

potential forming reactions are also given in Table 5.

Table 5

**Standard integral thermodynamic functions of the GeSe₂,
GeTe, Ag₈GeTe₆ compounds and Ag₈GeTe_{6-x}Se_x solid solutions**

Phase	$\Delta_f G^0$ (298 K)	$\Delta_f H^0$ (298 K)	$\Delta_f S^0$ (298 K)	S^0 (298 K)
	kJ·mol ⁻¹		J·K ⁻¹ ·mol ⁻¹	
*GeTe	52.87±0.09	49.5±0.4	11.3±1.0	91.1±1.4
*GeSe ₂	101.3±2.9	102.3±2.6	-	112.6±3.4
Ag ₈ GeTe ₆	234.8±0.5	217.5±2.7	58.0±7.6	726.0±10.0
Ag ₈ GeTe ₅ Se	263.6±1.9	241.7±3.6	73.5±8.5	734.2±10.2
Ag ₈ GeTe ₄ Se ₂	291.9±3.3	267.1±4.8	83.2±10.1	737.5±11.5
Ag ₈ GeTe ₃ Se ₃	301.1±3.4	269.3±4.9	106.7±10.2	753.7±11.8
Ag ₈ GeTe ₂ Se ₄	305.3±3.4	267.1±5.0	128.1±10.2	767.2±11.7
Ag ₈ GeTeSe ₅	307.2±3.4	265.4±5.0	140.2±10.8	772.8±12.5
β-Ag ₈ GeSe ₆	304.9±3.6	270.7±4.2	114.7±12.1	740.9±13.8

*Note: the quantities given for these compounds are literature data.

In the potential-forming reactions for solid solutions, the Te_{0.75}Se_{0.25}, Te_{0.5}Se_{0.5}, and Te_{0.25}Se_{0.75} solid solutions of the Te-Se system take part. According to the literature data given and explained in detail in the dissertation, the heat of mixing of these solid solutions is practically zero, that is, they are solutions very close to ideal. Therefore, in the calculations based on the potential-forming reactions, the values of the entropies of mixing and the Gibbs free energies of mixing these solid solutions were considered ideal solutions. Errors in all calculations were found by summing the errors.

RESULTS

1. The Ag, B^{IV} ||X, Te (B^{IV}- Si, Ge; X- S, Se) reciprocal systems were comprehensively studied along the 6Ag₂X+Ag₈B^{IV}Te₆ ↔ 6Ag₂Te+Ag₈B^{IV}X₆ compositions regions using differential thermal analysis, X-ray diffraction analysis, scanning electron microscopy, and also by EMF measurements of concentrations cells with Ag⁺ conductive solid electrolyte, and the nature of their physicochemical interaction in a wide temperature range was determined [1-3,5-9, 11, 13-17].

2. It has been shown that in the silicon-based reciprocal systems, the Ag_8SiS_6 - Ag_8SiTe_6 and Ag_8SiSe_6 - Ag_8SiTe_6 sections are quasi-binary and form continuous solid solution series between the high-temperature cubic modifications of the initial compounds. The corresponding sections of the germanium-based systems are partially quasi-binary due to the incongruent melting of the Ag_8GeTe_6 compound. However, they are also stable in the subsolidus and form continuous cubic solid solutions. The formation of solid solutions on all these sections is accompanied by a sharp decrease in the polymorph transformation temperatures of sulfide and selenide compounds and an expansion of the homogeneity regions of the high-temperature ion-conducting cubic phases over wide composition intervals to room temperature and lower temperatures [1,2, 11, 13, 14].
3. A complete scheme of phase equilibria in the $6\text{Ag}_2\text{S}(\text{Se})+\text{Ag}_8\text{SiTe}_6\leftrightarrow 6\text{Ag}_2\text{Te}+\text{Ag}_8\text{SiS}_6(\text{Se}_6)$ reciprocal systems in condensed states over a wide temperature range was obtained. Several polythermal and isothermal sections of the volume T-x-y diagram of both systems, as well as projections of liquidus surfaces, were constructed, and the non- and monovariant equilibria, the initial crystallization areas of the phases, and phase transformations occurring in the subsolidus were determined [1, 5, 6, 11, 14, 16, 17].
4. The $6\text{Ag}_2\text{Se}+\text{Ag}_8\text{GeTe}_6\leftrightarrow 6\text{Ag}_2\text{Te}+\text{Ag}_8\text{GeSe}_6$ reciprocal system was also fully studied, the projection of the liquidus surface onto the concentration triangle, the phase diagram, isothermal sections at temperatures of 300 and 500 K, as well as four vertical sections were constructed. In the $6\text{Ag}_2\text{S}+\text{Ag}_8\text{GeTe}_6\leftrightarrow 6\text{Ag}_2\text{Te}+\text{Ag}_8\text{GeS}_6$ system, the nature of the solid-phase equilibria at 300 K was determined [2,3,7-9,13,15].
5. It is shown that all the systems studied are reciprocal, i.e. they do not have quasibinary or stable diagonals. This can be explained by the presence of a large solid solution on the $\text{Ag}_2\text{S}(\text{Se})$ - Ag_2Te and $\text{Ag}_8\text{B}^{\text{IV}}\text{S}_6(\text{Se}_6)$ - $\text{Ag}_8\text{B}^{\text{IV}}\text{Te}_6$ boundary side of the concentration squares of these systems and the fact that they play a

decisive role in the formation of phase regions, and not the initial compounds [3, 7-9, 15, 17].

6. The characteristic feature of the studied reciprocal systems is that their liquidus surfaces are relatively simple in structure, reflecting the initial crystallization of 2-3 phases, while in the subliquidus and subsolidus regions, complex phase equilibria are observed due to the polymorphism of binary and ternary compounds and solid solutions based on them [7-9, 15].
7. Based on the constructed phase diagrams, new argyrodite phases with variable composition, including potentially mixed ion-electron conductive cubic phases with different compositions, discovered in the studied systems, were individually synthesized and identified. Their crystal lattice types and parameters were determined, and it was shown that the latter satisfy the Vegard rule [1,2, 6, 10, 11, 13, 14].
8. Using Ag_4RbI_4 superionic conducting solid electrolyte, concentration cells concerning the silver electrode were assembled, and Ag_8GeTe_6 compound and $\text{Ag}_8\text{GeSe}_{6-x}\text{Te}_x$ solid solutions were studied by EMF measurements in the 300-430 K temperature range. Based on those measurements, the partial molar functions of silver in alloys standard thermodynamic functions, and standard entropies of the mentioned compounds and phases were determined [4, 10, 12].

The results of the dissertation work were published in the following scientific works.

1. Y.Ə.Yusibov, A.C.Hüseynova, İ.C.Alverdiyev, M.B.Babanlı, Ag_8SiSe_6 - Ag_8SiTe_6 sistemində faza tarazlıqları /"Müasir təbiət və iqtisad elmlərinin aktual problemləri" beynəlxalq konfrans, Gəncə, 2018, s.3-4
2. Əmiraslanova A.C., İ.C.Alverdiyev, Y.Ə.Yusibov, M.B.Babanlı. Ag_8GeSe_6 - Ag_8GeTe_6 sistemində yeni dəyişən tərkibli fazalar / Müasir təbiət və iqtisad elmlərinin aktual problemləri, Gəncə, 2019, s. 3-5
3. Amiraslanova A.C., Məmmədova A.T., Alverdiyev İ.C., Yusibov

- Y.Ə $6\text{Ag}_2\text{Se} + \text{Ag}_8\text{GeTe}_6 \leftrightarrow 6\text{Ag}_2\text{Te} + \text{Ag}_8\text{GeSe}_6$ sisteminin 300 və 500 K-də faza diaqramları/ Müasir təbiət və iqtisad elmlərinin aktual problemləri, Gəncə, 2020, s. 28-31
4. Alverdiyev I.J., Amiraslanova A.J., Mashadiev L.F., Yusibov Y.A. Phase equilibrium in the reciprocal system Ag, Ge || Se, Te / 9th Rostocker International Conference: "Thermophysical Properties for Technical Thermodynamics", Rostock, Germany, 2020, p.65
 5. A.J.Amiraslanova, K.N. Babanlı, I.J.Alverdiyev, Y.A.Yusibov. New variable composition phases in the reciprocal system Ag, Si || Se, Te // "Физико-химические процессы в конденсированных средах и на межфазных границах", Воронеж, 2021, p.167-169
 6. Əmiraslanova A.C., Babanlı K.N., Alverdiyev I.J., Yusibov Y.Ə. $\text{Ag}_8\text{SiS}_6(\text{Se}_6)\text{-Ag}_8\text{SiTe}_6$ sistemlərində faza tarazlıqları / Müasir təbiət və iqtisad elmlərinin aktual problemləri, Gəncə, 2021, I hissə, s.3-5
 7. Əmiraslanova A.C., Alverdiyev İ.C., Yusibov Y.Ə., Babanlı M.B. $6\text{Ag}_2\text{Se} + \text{Ag}_8\text{GeTe}_6 \leftrightarrow 6\text{Ag}_2\text{Te} + \text{Ag}_8\text{GeSe}_6$ sisteminin likvidus səthi // Kimyanın müasir problemləri" respublika elmi konfransı, 2021, №1, s.81-82
 8. Yusibov Y.Ə., Əmiraslanova A.C., Məmmədova A.T., Alverdiyev İ.C. $6\text{Ag}_2\text{Se} + \text{Ag}_8\text{GeTe}_6 \leftrightarrow 6\text{Ag}_2\text{Te} + \text{Ag}_8\text{GeSe}_6$ sisteminin T-x-y diaqramı və onun bəzi izotermik kəsikləri / Müasir təbiət və iqtisad elmlərinin aktual problemləri, Gəncə, 2022, s.15-18
 9. Amiraslanova A.J., Mammadova A.T., Imamaliyeva S.Z., Alverdiyev I.J., Yusibov Yu.A., Babanlı M.B. The $6\text{Ag}_2\text{Se} + \text{Ag}_8\text{GeTe}_6 \leftrightarrow 6\text{Ag}_2\text{Te} + \text{Ag}_8\text{GeSe}$ reciprocal system // Russian Journal of Inorganic Chemistry, 2023, v.68, №8, p.1054-1064,
 10. Amiraslanova A.J., Mammadova A.T., Imamaliyeva S.Z., Alverdiyev I.J., Yusibov Yu.A., Babanlı M.B. Thermodynamic investigation of Ag_8GeTe_6 and $\text{Ag}_8\text{GeTe}_{6-x}\text{Se}_x$ solid solutions by the emf method with a solid Ag^+ conducting electrolyte // Russian Journal of Electrochemistry, 2023, №12, p.1071-1079
 11. Amiraslanova A.J., Babanlı K.N., Imamaliyeva S.Z., Yusibov Yu.A., Babanlı M.B. Phase equilibria in the $\text{Ag}_8\text{SiSe}_6\text{-Ag}_8\text{SiTe}_6$

- system and characterization of solid solutions $\text{Ag}_8\text{SiSe}_{6-x}\text{Te}_x$ // Applied Chemical Engineering, 2023, Vol 6, Issue 2, p.1-9.
12. Амирасланова А.Дж., Имамалиева С.З., Алвердиев И.Дж., Юсиров Ю.А. Термодинамические свойства теллурида серебра-германия // Гәnc тәdqiqatçı, 2023, Cild IV, №1, s.21-28
 13. Amiraslanova A.J., Mammadova A.T., Alverdiyev I.J., Yusibov Yu.A., Babanly M.B. $\text{Ag}_8\text{GeS}_6(\text{Se}_6)$ - Ag_8GeTe_6 Systems: phase relations, synthesis, and characterization of solid solutions. // Azerbaijan Chemical Journal. 2023, №1, p.22-29
 14. Amiraslanova A.J., Babanly K.N., Imamaliyeva S.Z., Alverdiyev I.J., Yusibov Yu.A. Phase relations in the Ag_8SiS_6 - Ag_8SiTe_6 system and characterization of solid solutions // Azerbaijan Chemical Journal. 2023, №2, p.169-177
 15. Amiraslanova A.J., Babanly K.N., Imamaliyeva S.Z., Alverdiyev I.J., Yusibov Yu.A., Babanly M.B. Phase relations in the $6\text{Ag}_2\text{Se}+\text{Ag}_8\text{SiTe}_6 \leftrightarrow 6\text{Ag}_2\text{Te}+\text{Ag}_8\text{SiSe}_6$ reciprocal system // Azerbaijan Chemical Journal. 2023, №3, p.6-17
 16. Амирасланова А.Дж., Бабанлы К.Н., Имамалиева С.З., Алиев И.И., Юсиров Ю.А. Твердофазные равновесия во взаимной системе $\text{Ag, Si} \parallel \text{S, Te}$ при 800 и 300 к / XII Международная научная конференция «Кинетика и механизм кристаллизации. Кристаллизация и материалы нового поколения», Иваново, 2023, с.61-62
 17. Əmiraslanova A.C., Məmmədova A.T., Alverdiyev İ.C., Yusibov Y.Ə $6\text{Ag}_2\text{Se}+\text{Ag}_8\text{SiTe}_6 \leftrightarrow 6\text{Ag}_2\text{Te}+\text{Ag}_8\text{SiSe}_6$ sistemində bərkfaza tarazlıqları / Müasir təbiət və iqtisad elmlərinin aktual problemləri, Gəncə, 2023, s. 3-5



The defense will be held on 27 February 2025 at 10⁰⁰ at the meeting of the Dissertation Council ED 1.15 of the Supreme Attestation Commission under the President of the Republic of Azerbaijan operating in the Institute of Catalysis and Inorganic Chemistry named after acad. M.Nagiyev of the Ministry of Science and Education of the Republic of Azerbaijan.

Address: H.Javid ave., 113, AZ-1073, Baku, Azerbaijan

E-mail: kqki@kqki.science.az

The dissertation is accessible at the library of the Institute of Catalysis and Inorganic Chemistry named after acad. M.Nagiyev of the Ministry of Science and Education of the Republic of Azerbaijan.

Electronic versions of the dissertation and its abstract are available on the official website of the acad.M.Naghiyev Institute of Catalysis and Inorganic Chemistry www.kqkiamea.az

The abstract was sent to the required addresses on 27 January 2025

Signed for printing: 23.01.2025

Paper format: 60x84^{1/16}

Volume: 38084 characters

Number of hard copies: 20